ICFM6
6TH INTERNATIONAL CONFERENCE ON FLOOD MANAGEMENT
September 2014 - São Paulo - Brazil

SEASONAL PROBABILISTIC FORECAST OF TROPICAL CYCLONE ACTIVITY IN THE NORTH INDIAN OCEAN

A. Espejo[1], F.J. Mendez[1], J.Diez[1], R. Medina[1], S. Al-Yayai[2]
1. *Environmental Hydraulics Institute "IH Cantabria" Universidad de Cantabria, Spain*
2. *Public Authority for Civil Aviation (PACA), National Meteorological Service, Oman*

ABSTRACT: Coastal flooding risk associated to tropical cyclones (TCs) is nowadays a major concern in low-lying and populated areas of the North Indian Ocean (NIO). In the past few years there have been devastating examples (i.e., Gonu or Phet in the Arabian Sea, and Nargis and Layla in the Bengal Bay) that encourages better understanding and predicting the activity of such events. Seasonal forecasting TC activity would lead to a more efficient coping these phenomena and mitigate its destructive effects.

It is well known that the TC genesis is boosted by warm sea surface temperature (SST), low to moderate vertical wind shear and upper level divergence. In this study we focus in the role of the SST as a needed precondition for TCs intensification with a twofold objective: (a) to define a statistical downscaling model to establish a relationship between large scale SST configurations and the occurrence probability of TCs; (b) to probabilistically forecast the occurrence rate of TCs in the NIO based on operational SST forecasts.

To build the statistical downscaling model, Y=f(X), we apply a combination of the principal component analysis and the k-means classification algorithm in order to identify representative patterns of large scale SST (predictor X) and the associated TC activity in terms of occurrence rate and expected tracks (predictand Y). Once explored the existing relations, we make use of the different runs of the NCEP's operational forecast, Climate Forecast System v2 (CFSV2). By using different runs we are able to construct an ensemble forecast (probabilistic) of the TC activity for the next month/season. The proposed model reveals that this approach provides complementary and useful information for a very early TC warning system.

Key Words: clustering algorithm, seasonal forecast, sea surface temperature, tropical cyclones

1. INTRODUCTION

Tropical cyclones are the most destructive weather phenomena to impact in tropical regions. In the NIO (Arabian Sea and Bay of Bengal) TCs are about 7% of the world's total and the intensity of these cyclones is moderated compared to typhoons/hurricanes. Nevertheless the NIO low-lying areas are one of the most vulnerable compared with other basins (Mandal, 2007; Mohanty, 2012). The year-to-year impacts vary, and historical records demonstrate significant inter-annual variability in TC frequency-intensity and spatial distribution of the TC tracks. Currently, there exists no operational seasonal TC prediction system over the region which could allow meteorological services to provide reliable advisories to the relevant national crisis management agencies. Thus, a reliable seasonal prediction of the TC activity is important for preparedness of coastal communities of the NIO. Over recent decades, statistical model-based methods for prediction of TC activity in the coming season have been developed for a number of regions. Statistical models use to explore relationships between large-scale drivers such El Niño-Southern Oscillation that modulates TC frequency, intensity and preferred tracks in some regions (Pielke and Landsea, 1999; Polgetier et al., 2005). One of the main limitations of the statistical models is the big amount of data needed to establish consistent relationships between the predictor (large scale driver) and the predictand (TC tracks), but also that the response of the predictand regarding the value of the predictor is not always linear.

It is well-known that the intensity of TCs is quite sensitive to the SST, which mainly determines the surface energy transfer from the ocean. A number of studies confirm that warm local SST (≥26ºC) is one of the necessary conditions for the genesis and intensification of TCs (Palmen, 1948; Gray, 1968; Emanuel, 1987). The goal of our work is based on the idea of data mining which comprises a set of algorithms allowing an objective classification of *M* SST fields in the NIO. Each SST configuration is linked to a specific behavioral pattern of the TCs. Thus, by using different runs of the CFSv2, and determining what SST pattern is the nearest to each run, we are able to construct an ensemble forecast of the TC activity for the next season. A schematic diagram of the framework is displayed in Figure 1.

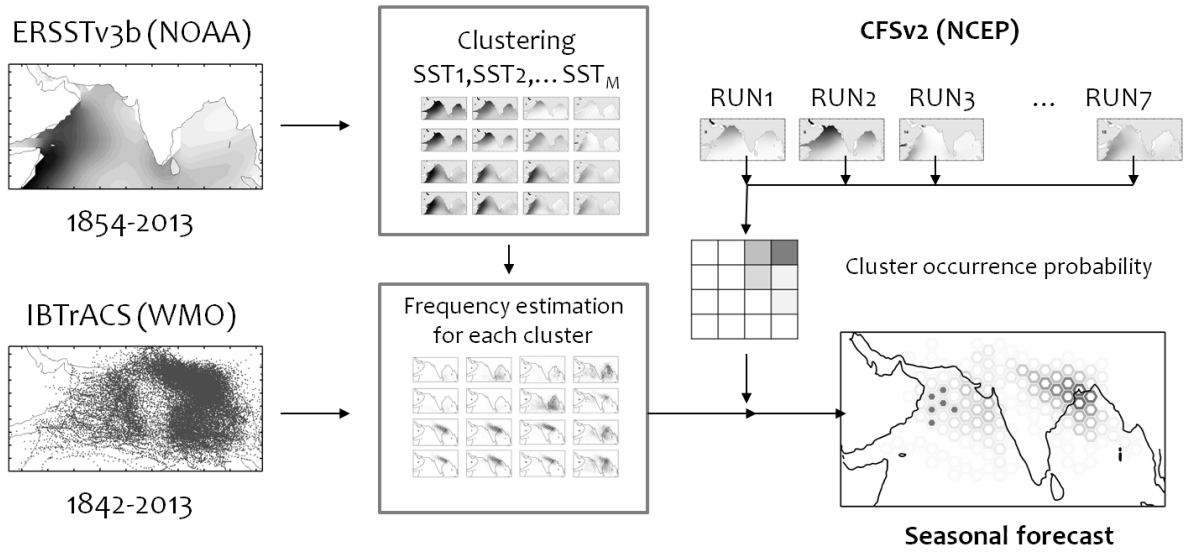

Figure 1: Schematic diagram of the clustering-based forecast system. From each 7 runs, the nearest SST cluster is determined, final forecast for one month/season is obtained by summing the product of the probability of the forecasted SST to belong to one cluster with the TC frequency of each cluster.

The paper is organized as follows. Section 2 describes the data used to train the model (SST and TC tracks) and presents a brief description of the CFSv2 seasonal forecast. In Section 3 the statistical downscaling and the forecast system are described. As an example, the forecast for the current and the following three months are presented in Section 3. This is followed by the conclusions in the final section.

2. DATA

In order to construct our predictor we use monthly mean SST data for the period 1854 through 2013 derived from NOAA Extended Reconstruction Sea Surface Temperature version 3b (ERSSTv3b ,Smith et al., 2003). The chosen domain covers the NIO between 40ºE and 10ºW and between 0ºN and 30ºN with a 2 degree regular grid. Although inconsistencies appear prior to 1900 due to the scarcity of the data and the method of reconstruction, we have used the whole period to perform our analysis. The ERSST provides global, spatially complete SST data at a monthly basis. It is based upon statistical interpolation of the ICOADS release 2.4 data. Version 3b does not include satellite data due to a cold bias in the satellite-derived SST.

Besides atmospheric conditions, it is recognized in the literature that the cyclone characteristics related to maximum wind speeds and minimum pressures are dependent on SST and, for this reason, we check that all sampled tracks hold a limiting condition in terms of the SST at the track position. If we take the pressure associated with each historical cyclone track in mbar and its corresponding SST in Celsius degrees, and plot the standardized pressure deficit, MDi versus SSTi, the graph shown in Figure 2 is

obtained. Note that maximum deficits occur for sea surface temperatures between 28ºC and 30ºC with a maximum in about 29ºC. For this reason, and with the intention of optimizing the information used as input in the clustering algorithm, we use the transformed SST named sea surface temperature index, ISST. This transformation tries to capture those SST situations in which a TC can intensify, the envelope shown in Figure 2 is obtained by means of the expression,

$$ISST = \left(1 - \left(\frac{SST - 29}{3}\right)^2\right)^3$$

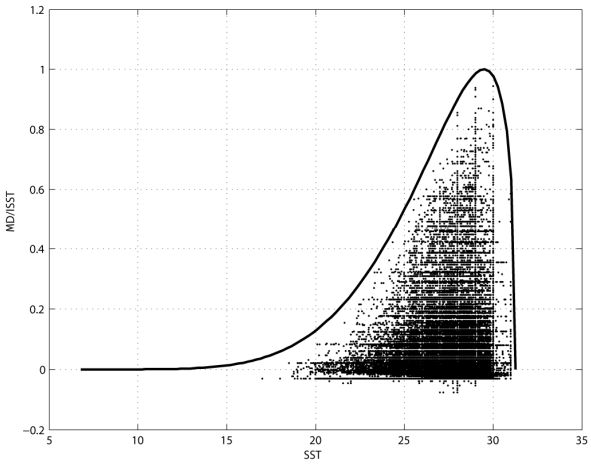

Figure 2: Maximum normalized pressure deficits MD versus SST.

To accurately assess the relations between TC activity and SST configuration a long, reliable and homogeneous observational TC track dataset in the NIO is needed. At the time, the IBTrACS dataset (International Best Track Archive for Climate Stewardship; Knapp et al., 2010) is the most complete archive of TCs because it merges storm information from multiple climate centers. IBTrACS time coverage spans from 1842 to 2013, offering TC tracks with a 6 hours time step. For analysis purposes, the 6-hourly data have been interpolated to hourly intervals using the method outlined in Elsner and Jagger (2012). Although, in the early period there is only the position of the TC tracks with rough information about maximum wind speed and minimum pressure, these data are very useful since we are not only interested in properly characterize the TC intensities but also the TC preferential tracks under one or another SST configuration.

The coupled general circulation model used for the development of the seasonal TC forecasting system is the latest version of National Centers for Environmental Prediction (NCEP) CFSv2 (Saha et al. 2013,2014) which is run at T126 (~100km) and T382 (~38 km) horizontal resolutions with 64 vertical levels and forced with bias corrected daily SST. The atmospheric component of the model is the NCEP GFSv2 at T126 resolution which is coupled to the GFDL Modular Ocean Model version 4p0d (MOM4; Griffies et al. 2004), sea-ice model and land surface model. MOM4 has zonal resolution of 1/2° and meridional resolution of 1/4° between 10°S and 10°N, gradually increasing through the tropics to 1/2° pole ward of 30°S and 30°N. There are 40 layers in the vertical with 27 layers in the upper 400 m of the ocean, and the maximum depth is approximately 4.5 km. The vertical resolution is 10 m from the surface to 240 m depth, gradually increasing to about 511 m in the bottom layer.

The CFSv2 SST outputs are as follow (see Figure 3): there are 4 control runs per day from the 0, 6, 12 and 18 UTC cycles of the Climate Forecast System using the real-time data assimilation system and

going out to 9 months; in addition to the control run of 9 months at the 0 UTC cycle, there are 3 additional runs, out to one season; in addition to the control run of 9 months at the 6, 12 and 18 UTC cycles, there are 3 additional runs, out to 45 days. Finally there are available a total of 16 CFS runs every day, of which 4 runs go out to 9 months, 3 runs go out to 1 season and 9 runs go out to 45 days. This scheme rules the time-span of the forecast, in which we only dispose of a maximum number of members of 7 for the monthly ensemble forecast (3 seasonal forecasts at the 0 UTC run plus 4 control 9 month runs at 0, 6, 12 and 18 UTC).

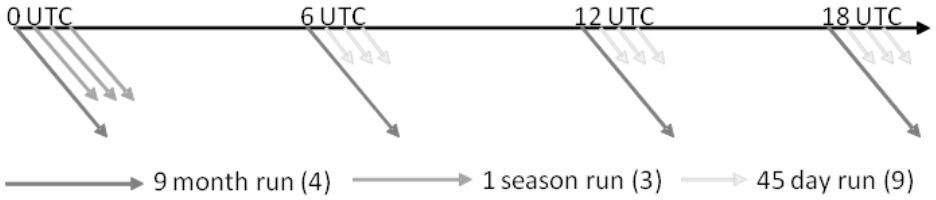

Figure 3: Operational CFSv2 configuration.

3. METHODOLOGICAL FRAMEWORK

3.1 STATISTICAL DOWNSCALING/TRAINING THE MODEL

Traditional approaches for characterizing NIO SST variability are based on one-dimensional indices such as the Indian Ocean Dipole (IOD; Saji et al., 1999), assuming linear climatic responses depending on the value of this SST based climate index. When using nonlinear clustering techniques it is possible to objectively distinguish different groups within the continuous tropical SST variability which may be linked to specific responses or climate anomalies such as the TC activity. Each one of these groups must contain statistically homogeneous SST fields and statistically different from the SST fields contained in the remainder groups. Today, a wide variety of clustering algorithms can be found in the field of data mining. Their conceptual principle is maximizing similarity within groups while maximizing dissimilarity between groups. Standard methods in data mining include: the k-means algorithm (Hastie et al., 2001) and the self-organizing maps (Kohonen, 2000). Basically they can be distinguished because of the method for determining distances and the topological neighborhood imposed conditions. Both algorithms have been recently applied for different geophysical spatial fields (Gutierrez et al., 2005; Reusch et al., 2007; Polo et al., 2011; Izaguirre et al., 2012; Guanche et al., 2013). Camus et al., 2011 compared the k-means and SOM clustering skills when working with multivariate wave climate. They found that SOM is the best technique to graphically characterize a multi-dimensional variable: results can be projected in a two-dimensional lattice allowing an easy visualization of highly dimensional patterns. Whereas SOM technique is constrained by the neighborhood conditions and the relative density of the data (i.e., SOM clusters tend to cover more effectively mean conditions where data density is higher), k-means is not, and thus, they concluded that k-means perform a better classification in terms of mean errors within the group.

In order to find synoptic ISST patterns in the tropical Pacific, the k-means clustering algorithm is applied. We initialize the search of clusters with the deterministic maximum dissimilarity method (Camus et al., 2011). For a better clustering performance, ISST fields have been previously transformed into spatial and temporal modes using Principal Components Analysis (PCA), thus reducing the high-dimensionality of the original data space. Results consist of a number of clusters, each one defined by a prototype and formed by the data for which the prototype is the nearest (Hastie et al., 2001). The data is composed of $N = 159 \times 12 = 1908$ monthly ISST fields, $\{ISST(x,t_1), ISST(x,t_2), ..., ISST(x,t_3)\}$,where x represents each ocean location (496 grid points) and t is time in months (t_1 is the first month, January 1854, and t_N is the last month, December 2013). We first apply PCA capturing the n first modes that explain 99% of data variability (n=9 in this work), obtaining the eigen orthogonal functions, $\{EOF_1(x), EOF_2(x), ..., EOF_N(x)\}$, and their associated temporal amplitudes, or principal components, $\{PC_1(t), PC_2(t), ..., PC_N(t)\}$. Second, k-means

algorithm is applied to the *N* multivariate data (n-dimension), $\{PC_1(t), PC_2(t), ..., PC_N(t)\}; t = 1, ..., N$; obtaining *M* groups or ISST types defined by a prototype or centroid for each kth-cluster, as $ISST_k = \{PC_{1,k}, PC_{2,k}, ..., PC_{n,k}\}; k = 1, .., M$. After that, considering the spatial modes (EOFs) corresponding to each PC, the centroids are expressed in the original space for the kth-cluster as $ISST_k(x) = \{EOF_1(x)PC_{1,k} + EOF_2(x)PC_{2,k} + ... + EOF_n(x)PC_{n,k}\}; k = 1, .., M$. The number of clusters *M* is chosen following the criteria of representativeness of the cluster (mean number of elements in each group). In our work we have used a classification with M=16 clusters, with an average number of 120 elements in each group. Figure 4 displays the result of the classification in the first three PCs space, as can be seen, the obtained centroids satisfactory span over the wide variability of the data..

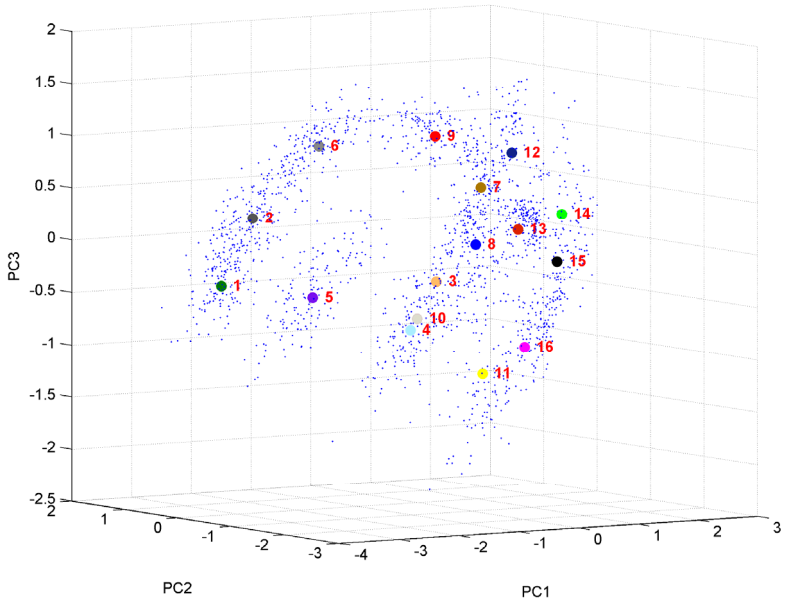

Figure 4: ISST data into the PC space. Small blue dots represent the monthly ISST as function of the first 3 PCs. The numbered solid (colored) dots represent the M=16 clusters obtained using k-means algorithm initialized with maximum dissimilarity algorithm.

Once the centroids are obtained, making use of the minimum distance criteria, the method is able to identify the most similar cluster to each monthly ISST, thus constructing a date vector for each cluster. Using this date vector is easy to identify those TCs occurring simultaneously to one or another ISST type. For this procedure, we have selected the date of maximum intensity of each TC to allocate it into one ISST type. Figure 5 represent the 16 ISST types with its corresponding TC tracks. As can be seen, most of the tracks represent tropical depressions to tropical storms, especially those occurring on the left side of the lattice (ISST types 1 to 8). It is to mention how cyclones born and propagate throughout the darker zones of each panel. Most of the ISST types appearing in left side are characterized by typical out of TC season SST configurations. As for example ISST types 1 and 2 that only appear in January and February (see Figure 7). Nevertheless, in the right upper corner a set of ISST types with suited SST configuration for the TC genesis and intensification can be observed. TCs reaching at least category 3 only take place in the SST types 9, 10, 12, 13, 14 and 15. Within these types it is possible to differentiate those giving advantage to the TCs of the Arabian Sea (ISST types 13 and 14) and those favoring the TC activity in the Bengal Bay. It should be pointed that Gonu and Phet (June, 2007 and 2010), two of the most intense cyclones on record in the Arabian Sea, took place under the ISST type 14. The predictive character of the ISST configuration is evidenced due to the fact that the classification is able to discern not only between TC intensities but also between preferred tracks.

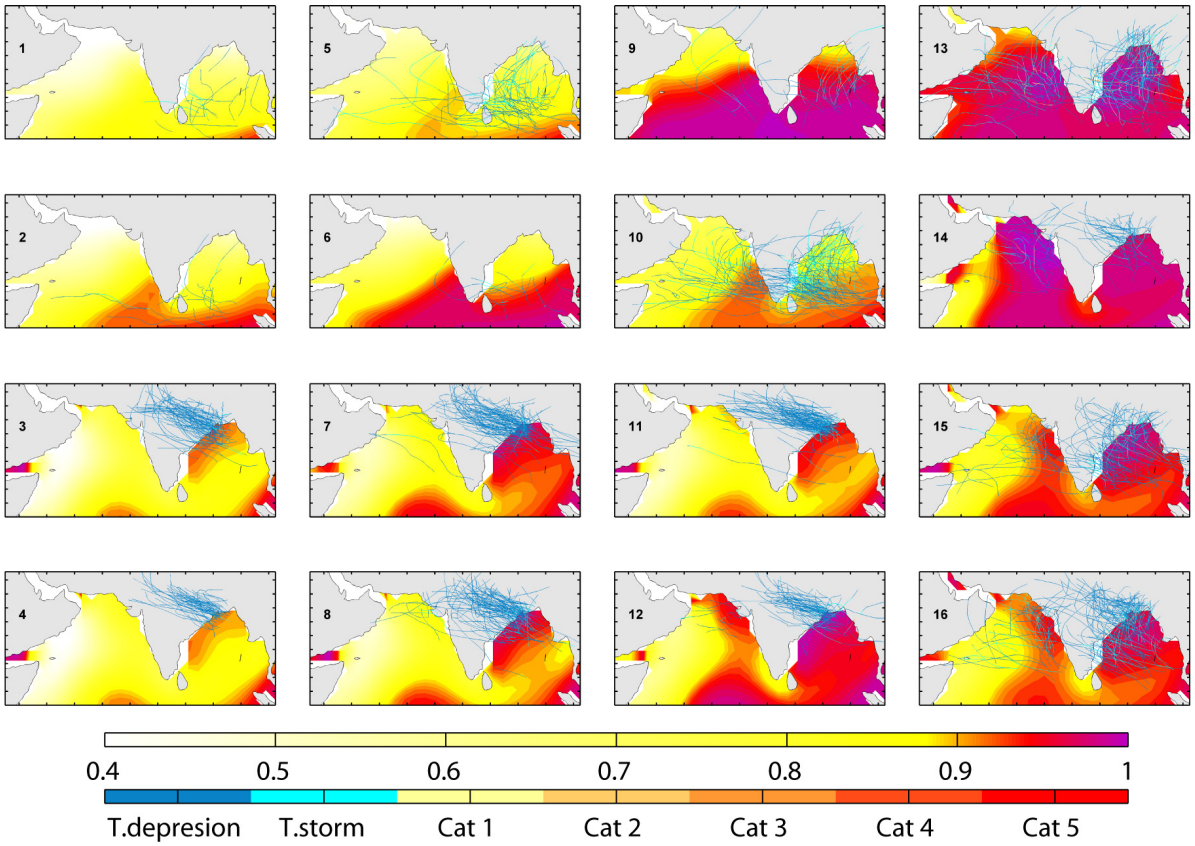

Figure 5: M=16 ISST types and corresponding TC tracks (colors correspond to the ISST values and the Saffir-Simpson scale).

TC differences between the M=16 types are more easily appreciable when looking at Figure 6, in which the probability of having a tropical depression or higher in the Saffir-Simpson scale is shown in the blue color scale and the probability to be over category 3 or higher is expressed in the red color scale. The probabilities shown in Figure 6 correspond to the monthly frequency (in %) of the TC occurrence into a hexagonal grid defined in a Mollweide projection ensuring equal area polygons (see Elsner et al., 2012). The selected area (50.000 km^2) is sufficiently small to discern the preferred track at a regional scale and sufficiently big to capture enough TCs. Cyclone counts have been made as function of the number of cyclones that passed through each hexagon (one count for each TC). By means of this spatial discretization several differential TC behavior come out. As for example the low occurrence rate of TCs in types 1, 2 and 6 or the wide spread tracks appearing on the forth column. It is worthwhile to note the marked preferred tracks (southeast-northwest) with a common genesis zone on the upper margin of the Bengal Bay. These more usual tropical depressions or storms differ from those more intense (category 3 or higher) not only in the genesis area (usually low latitudinal) but also in the course they tend to take, with tracks going from south to northeast. This is the case of the low latitude cyclone Nargis, what made landfall in Myanmar on Friday, 2 May 2008. Moreover, the idea that the TC activity tend to be more damaging in the Bengal bay or the Arabian Sea depending on the year seems to be supported by this classification, depending of the year dominance of type 13 or 14. In the same way, it should be noted that types encompassing enhanced TCs intensities tend to include less number of weak tropical systems (right upper corner of the lattice).

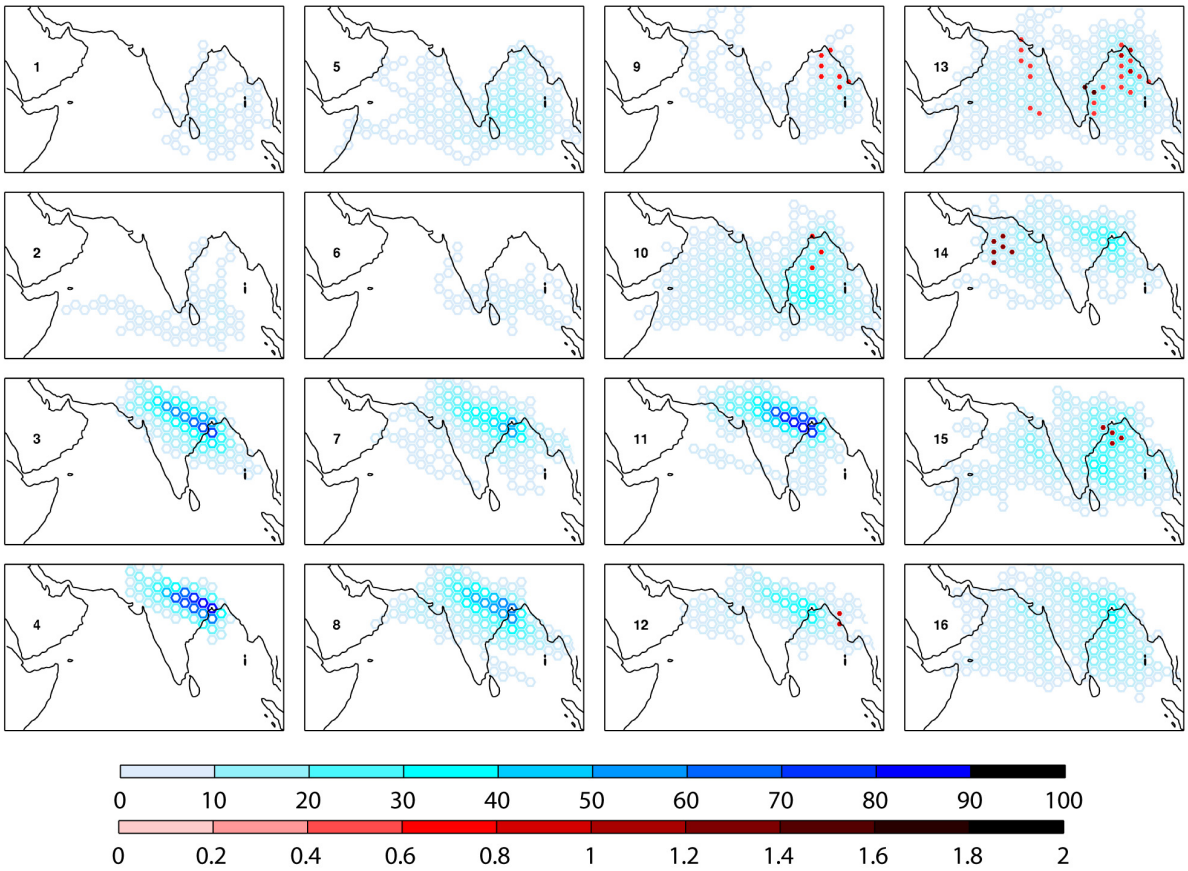

Figure 6: Monthly TC probability (in %) corresponding to each ISST type (blue colors). The red colors at the center of the hexagons indicate the relative probability of exceeding category 3.

As displayed in Figure 7 the ISST patterns occurrence present a clear seasonal pattern. Thus, the most frequent types appearing in the two peaked TC season in the NIO (April, May, June, October, November) are: 9, 13, 14, 15 and 10. The 3-year smoothed yearly occurrence of the ISST types is shown in the lower panel of Figure 7. Results indicate that type 1, corresponding to relative cold waters, is being substituted by the warmer type 2 (type 1 disappear since the 80's). On the other hand, types such as 12, 13 and 14, related with severe cyclonic activity are rising up. This fact explains the risen TC activity experienced in the NIO in the last years. If this activity is or not the result of the global warming is not the focus of this paper, nonetheless this fact agrees with the idea that warmer and moister environment would have an enhanced overall cyclone activity (Anthes et al., 2006). It is difficult to trust TC track datasets before the satellite era, so it is not convenient to link inter-annual variability of the ISST types occurrence with the TC activity. However, the observed trend in the occurrence of the active ISST types from 1980 explains the results obtained by Deo et al., 2011, arguing increased net TC activity.

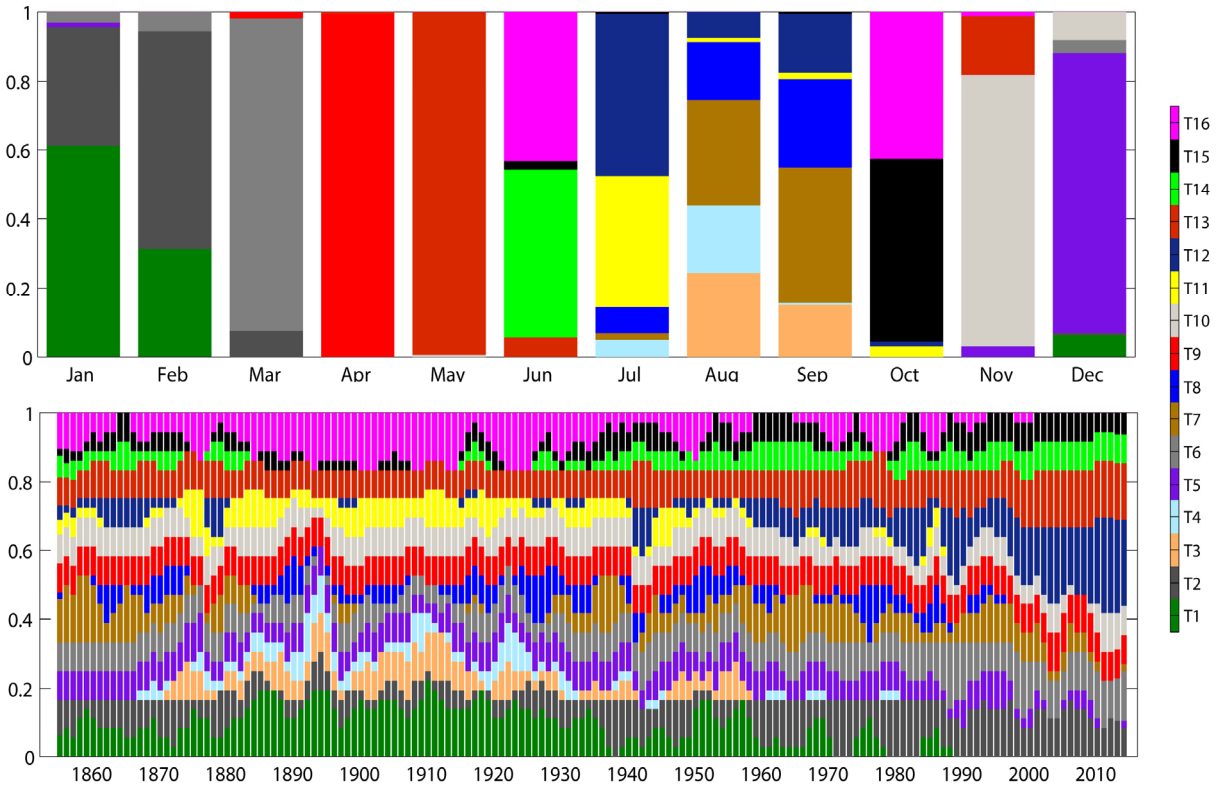

Figure 7: ISST seasonality (upper panel) and 3-year smoothed annual occurrence probability (lower panel).

3.2 FORECASTING

We use the CFSv2 operational system to obtain future monthly ISST fields for the statistical TC forecasting. Each day, 7 runs for each coming four months are downloaded (http://nomads.ncep.noaa.gov/pub/data/nccf/com/cfs/prod/cfs/) for the area of interest, interpolated to the original coordinates of the data used in the training stage, and transformed to ISST. Before projecting this ISST fields into the PC space, we have checked the ability of the CFSv2 to represent the relative frequency of the ISST types in the shared period with ERSST v3b (1980-2013) obtaining very good results (not shown here). This means that both SST databases are not biased and thus they can be inter-compared. The comparison is made in the PC space, so the forecasted ISST fields are previously expressed regarding the new coordinates or EOFs.

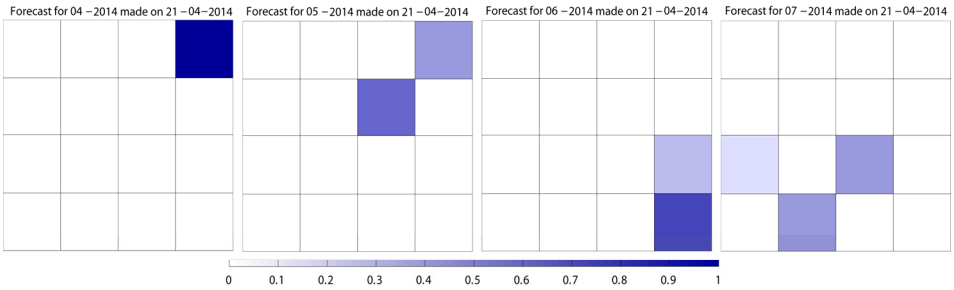

Figure 8: Probability of the 7 monthly runs (from left to right, April, May, June, July, 2014) to belong to one ISST type.

Figure 8 represent the probability of the forecasted ISST to belong to one of the clusters. As expected, the 7 runs for the current month (April) are quite similar between them, all being represented by one of the types. Going further in the forecast period, the obtained ISST fields began to be more different. In May, most of the runs go to types 10 (4 of the 7 runs), while in June and July the forecast is more uniformly distributed between two or more ISST types.

Making use of the probabilities displayed in Figure 6 and 8, it is possible to determine the probability of TCs for the next months. Figure 9 present the results obtained from April to July, 2014. As can be observed, April present the most dangerous forecast because the ISST filed for this month is quite similar to type 13 with high TC activity. Surprisingly to some extent, ISST 13 is very rare to occur in April. Nonetheless, May and June forecasts also indicate enhanced tropical activity, especially in the Bay of Bengal. This activity is expected to be suppressed in July, coinciding with the Southwest Monsoon onset.

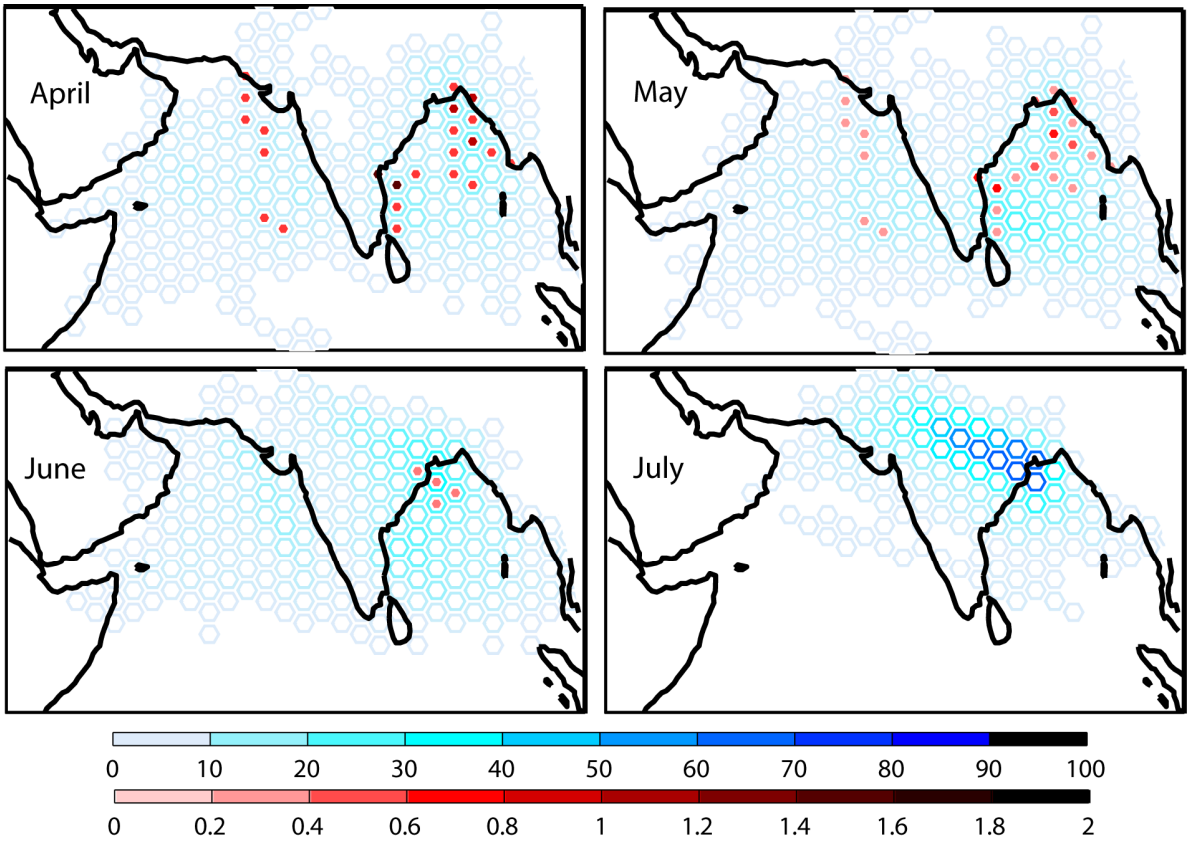

Figure 8: TC activity forecast for April-July, 2014. Results are expressed in %.

4. CONCLUSIONS

The inter-annual variability of the TC activity in the NIO is large (intensity and spatial distribution), being highly conditioned by the SST configuration. A better management of this year to year variability is essential to decrease current and future vulnerability to TCs. The proposed statistical forecast has proved to be an efficient method to forecast TC activity for the next few months. The method is based on relating TC activity and monthly SST configurations over the NIO. For this task we have used long-term time series for both the predictor and the predictand (more than 150 years). In order to better relate SST and TC activity we have previously transformed the net SST into and ISST index [0-1] which better capture the ranges of SST and TC intensity. Instead of using a derived SST index such El Niño or the IOD as most of the statistical forecast systems, we have used a clustered based method (k-means) to obtain

synoptic types of the ISST. By doing this we are able to hold nonlinear relations therefore improving those statistical forecasts based on linear relations. Apart of considering more complex predictors (vorticity, wind shear stress, etc) the ISST has proven to be quite related with the TC activity and thus it can be used as predictor. It should be mentioned that the major shortcoming of this approach is that the model cannot account for climate variability and change that are not represented in the historical record.

Once the relations are established we make use of the CFS v2 monthly forecast to extract SST configurations in the NIO. These SST fields are compared with those obtained with k-means classification indentifying the most similar one. Dynamical extended range prediction is subjected to various sources of errors, of which the errors arising from the uncertainties in the initial conditions and model are important. To eradicate such errors, ensemble prediction approach is one of the best options and has been attempted by various operational centers. As the CFS v2 launches a set of (7 daily runs per forecasted month) we can perform a probabilistic forecast. The skill of this method relies on the skill of the CFS v2 to properly forecast feasible and realistic SST fields in the NIO.

We believe that this work can ultimately provide valuable and applicable climate information about TC activity for the next future, which can help decision making, responses and adaptation in the most vulnerable areas. The next step toward improving skill of TC seasonal prediction in the NIO will be undertaken through validating the method using stored SST forecasts. This is particularly important to assess alarm levels under different kind of forecasts. Moreover incorporating more variables as predictors would lead to reduce uncertainness in the statistical downscaling technique.

5. REFERENCES

Anthes, R. A., R. W. Corell, G. Holland, J. W. Hurrell, M. C. McCracken, and K. E. Trenberth, 2006: Hurricanes and global warming—Potential linkages and consequences. Bull. Amer. Meteor. Soc., 87, 623–628.

Camus, P., F. J. Mendez, R. Medina, and A. S. Cofiño, 2011: Analysis of clustering and selection algorithms for the study of multivariate wave climate. Coastal Eng., 58, 453–462, doi:10.1016/j.coastaleng.2011.02.003

Deo A. A, D.W.Ganer and G. Nair, 2011: Tropical cyclone activity in global warming scenario, Natural Hazards , 59, 2, 771-786, DOI: 10.1007/s11069-011-9794-8

Elsner J. B. and T. H. Jagger, 2012: *Hurricane Climatology: A Modern Statistical Guide Using R*, Oxford University Press, 2013, 380pp.

Elsner, J.B., R. E. Hodges, and T.H. Jagger, 2012: Spatial grids for hurricane climate research. Clim. Dyn., 39(1), 21-26-

Emanuel, K.A., 1987: The dependence of hurricane intensity on climate. Nature, 326, 483-485.

Gray, W. M., 1968: Global view of the origin of tropical disturbances and storms. Mon. Wea. Rev., 96, 669-700.

Griffies, S. M., 2004: *Fundamentals of ocean climate models*. Princeton University

Guanche, Y., Mínguez, R., Méndez, F.J. 2013: Autoregressive logistic regression applied to atmospheric circulation patterns. Climate Dynamics http://dx.doi.org/10.1007/s00382-013-1690-3.

Gutiérrez, J.M., Cano, R., Cofiño, A.S., Sordo, C., 2005: Analysis and downscaling multi-model seasonal forescast in Peru using self-organizing maps. Tellus 57A, 435–447.

Hastie, T., Tibshirani, R., Friedman, J., 2001: *The Elements of Statistical Learning*. Springer, New York.

Izaguirre C., Menendez M., Camus P., Mendez F.J., Minguez R., Losada I.J. 2012: Exploring the interannual variability of extreme wave climate in the northeast atlantic ocean. Ocean Modelling, 59–60:31–40. http://dx.doi.org/10.1016/j.ocemod.2012.09.007

Knapp K.R., M.C. Kruk, D.H. Levinson, H.J. Diamond, and C.J. Neumann, 2010: The International Best Track Archive for Climate Stewardship (IBTrACS), Bulletin of the American Meteorological Society, vol. 91, pp. 363-376, 2010. http://dx.doi.org/10.1175/2009BAMS2755.1

Kohonen, T., 2000: *Self-organizing Maps*, 3rd ed. Springer-Verlag, Berlin Press.

Mandal M., U.C. Mohanty, P. Sinha and M. M. Ali, 2007: Impact of sea surface temperature in modulating movement and intensity of tropical cyclones by Natural Hazards, 41, 3, 413-427

Mohanty U.C., Niyogi D, Potty K.V.J., 2012: Recent developments in tropical cyclone analysis using observations and high resolution models, Natural Hazards, 63, 3, 1281-1283.

Palmén, E.H., 1948: On the formation and structure of tropical cyclones, Geophysica, 3, 26-38.

Pielke, R.A., Landsea, C.N., 1999: La Niña, El Niño, and Atlantic Hurricane Damages in the United States, Bull. Amer. Met. Soc., 2027-2033.

Polo, I., Ullmann, A., Roucou, P., Fontaine, B., 2011: Weather regimes in the euro-atlantic and mediterranean sector, and relationship with west african rainfall over the 1989–2008 period from a self organizing maps approach. J Clim 24:3423–3432

Potgieter, A.B., Hammer, G.L., Meinke, H., Stone, R.C., Goddard, L., 2005: Three Putative Types of El Niño Revealed by Spatial Variability in Impact on Australian Wheart Yield, J Clim, 18, 1566-1574.

Reusch, D.B., Alley, R.B., Hewitson, B.C., 2007: North Atlantic climate variability from a self-organizing map perspective. J. Geophys. Res. 112, D02104.

Saha, S. and Coauthors, 2010: The NCEP Climate Forecast System Reanalysis. Bull. Amer. Meteor. Soc., 91, 1015.1057. doi: 10.1175/2010BAMS3001.1

Saha, S. and Coauthors, 2014: The NCEP Climate Forecast System Version 2 Journal of Climate J. Climate, 27, 2185–2208. doi: http://dx.doi.org/10.1175/JCLI-D-12-00823.1

Saji, N. H., B. N. Goswami, P. N. Vinayachandran, and T. Yamagata, 1999: A dipole mode in the tropical Indian Ocean. Nature, 401, 360-363.

Smith, T.M., and R.W. Reynolds, 2003: Extended Reconstruction of Global Sea Surface Temperatures Based on COADS Data (1854-1997). *Journal of Climate*, 16, 1495-1510.